

Strategy to isolate ionic gold sites on silica surface: Increasing their efficiency as catalyst for the formation of 1,3-diynes

Cezar A. Didó^a, Felipe L. Coelho^a, Maurício B. Closs^a, Monique Deon^a, Flavio Horowitz^b, Fabiano Bernardi^b, Paulo H. Schneider^{a,*}, Edilson V. Benvenutti^{a,*}

^a Institute of Chemistry, UFRGS, CP 15003, CEP 91501-970, Porto Alegre, RS, Brazil

^b Institute of Physics, UFRGS, CP 15051, CEP 91501-970, Porto Alegre, RS, Brazil

ARTICLE INFO

Keywords:

Organic-inorganic hybrid composites
Sol-gel process
Gold
Alkynes
Cross-coupling
C-C coupling

ABSTRACT

A new strategy is presented to obtain an efficient heterogeneous gold catalyst constituted by isolated ionic gold sites, which is known to be effective in alkyne coupling reaction. The procedure is based on a significant difference between offered gold amount and available adsorbent sites on the support, ensuring the formation of very active isolated gold ion sites. In order to achieve this purpose, mesoporous silica xerogel was grafted with an ionic silsesquioxane containing charged ammonium quaternary group. The modified silica showed 0.25 mmol of cationic sites per gram of material and presented thermal stability up to 200 °C. This material was applied as support for immobilization of Au(III) ions as square planar AuCl_4^- complex. The gold amount offered was just 12 % of the exchangeable capacity. The catalyst was efficiently applied in the cross coupling reactions, in which only 0.22 mol% was applied to obtain symmetric and non-symmetric 1,3-diynes.

1. Introduction

Although gold is considered inert noble metal in the bulk form, it has emerged in the last decade as a powerful catalyst in reactions for organic transformations when used at the nanoscale or even lower [1–7]. Considering that heterogeneous catalysis allows the recovering of the catalyst, the development of gold catalyst dispersed in several porous inorganic supports has become important [8–12]. Among the inorganic supports, silica has been extensively employed because it can be easily synthesized by sol-gel process, with designed characteristics such as texture and morphology [12–15]. Additionally, silica presents intrinsic desired properties such as chemical, thermal and mechanical stability, even though, it enables surface functionalization by using grafting reactions [12,14,16].

Gold complex is a very efficient catalyst in several organic reactions [4,17] including the cross-coupling reactions of terminal alkynes to synthesize symmetric and non-symmetric products of 1,3-diynes [17–23]. These compounds present great relevance as building blocks and provide a large number of compounds in the chemical, pharmaceutical and materials industry. The success of gold complex as catalyst has been explained based on its redox potential Au(I)/Au(III) [6,20,24–27], however the precise nature of the redox process for gold chloride complex is not well established. [28–30].

A very common gold complex is the AuCl_4^- anion [31,32], which can be easily obtained by dissolving gold metal in *aqua regia* and, as far as we know, this complex has not been applied in coupling reactions of alkynes. This complex can be covalently immobilized on the surface of inorganic supports containing chelating groups, such as amine or sulfur [33–35]. Another way to immobilize this complex is by using the ion-exchange process, in which the inorganic matrix is previously modified with cationic organic sites, such as quaternary ammonium groups [12,36]. However, the immobilized gold complexes have a thermodynamic trend to aggregate and convert themselves into gold clusters or nanoparticles [12,31,34,37,38].

Aiming to avoid such aggregation, in the present work we have designed a catalyst containing a very small amount of isolated ionic gold sites on the silica surface. This aim was achieved by using a silica xerogel matrix that was previously functionalized with an ionic silsesquioxane. This charged compound is a hybrid oligomeric material that presents organic chain with quaternary ammonium group and it is covalently bonded to a silica moiety. This charged chain provides water solubility and ion exchange capacity. Furthermore, the silica part has silanol groups that undergo crosslink reactions and graft the silsesquioxane as films onto inorganic surfaces [39]. By using the ion-exchange process, AuCl_4^- complex was immobilized and the offered gold amount was much lower than the available cationic sites. The catalyst

* Corresponding authors.

E-mail addresses: Paulos@iq.ufrgs.br (P.H. Schneider), benvenutti@ufrgs.br (E.V. Benvenutti).

<https://doi.org/10.1016/j.apcata.2020.117444>

Received 14 November 2019; Received in revised form 30 January 2020; Accepted 31 January 2020

Available online 01 February 2020

0926-860X/ © 2020 Elsevier B.V. All rights reserved.

was efficiently applied in cross coupling reactions to obtain symmetric and non-symmetric 1,3-diynes.

2. Experimental section

2.1. Synthesis of the silsesquioxane (SSQ)

The procedure to obtain the ionic silsesquioxane was based on a previous report [40]. The 1,4-diazabicyclo[2.2.2]octane (Sigma-Aldrich, 6.0 g) and 12.2 mL of 3-chloropropyltrimethoxysilane (Aldrich) were dissolved in dimethylformamide (Sigma-Aldrich, 45 mL). The mixture was heated up to 76 °C under stirring and nitrogen atmosphere until a white solid precipitates. Then, this solid was washed with methyl alcohol and dried for 4 h at 50 °C. The solid was dissolved in 45 mL of formamide (Vetec), at 75 °C, under stirring. Afterwards, water (0.8 mL) and HF 40 % (Aldrich, 0.3 mL) were added. The gelation was carried out at 45 °C. The final white solid, the cationic silsesquioxane, was named as SSQ.

2.2. Synthesis of silica xerogel (SiO₂)

The SiO₂ was synthesized by sol-gel method. Tetraethylorthosilicate (Aldrich, 5.0 mL) was added to ethanol (Merck, 5.0 mL). After, 2.0 mL of distilled water containing 3 drops of hydrofluoric acid 40 % (Aldrich) were added. The system was stored for 14 days, at room temperature, for gelation and solvent evaporation. Subsequently, the resulting xerogel was washed with distilled water, ethanol, and dried under vacuum for 2 h.

2.3. Organofunctionalization of SiO₂ with ionic silsesquioxane (SiO₂/SSQ)

The SiO₂ material was organofunctionalized by grafting reaction. The SiO₂ (2.40 g) was added to an aqueous SSQ solution (0.96 g in 30 mL) and the mixture was stirred for 22 h at room temperature. Afterwards, the solid was separated from the supernatant and vacuum dried for 2 h at 80 °C. Then, the modified xerogel was washed using distilled water and ethylic alcohol, and vacuum dried at 75 °C for additional 2 h. The resulting modified xerogel was named as SiO₂/SSQ.

2.4. Immobilization of AuCl₄⁻ in organofunctionalized silica (SiO₂/SSQ/Au)

The SiO₂/SSQ material was submitted to ion-exchange process with AuCl₄⁻. The SiO₂/SSQ (2.41 g) was added to HAuCl₄ solution (4.10⁻³ mol·L⁻¹, 20 mL) previously prepared by dissolving 79 mg of gold powder (Vetec) in 4 mL of aqua regia (nitric acid 65 % (Aldrich) and hydrochloric acid 37 % (Merck), v/v 1:3) that were diluted to 100 mL with distilled water. The system was stirred for 2 h, and then the solid was separated from the supernatant, and vacuum dried for 3 h at ambient temperature. Finally, the resulting yellowish material was

purified by washing with distilled water and ethylic alcohol, and vacuum dried at ambient temperature for additional 3 h. This material was named SiO₂/SSQ/Au.

2.5. Characterization

UV-Vis spectrum of HAuCl₄ aqueous solution was recorded in a UV-160 1PC Shimadzu spectrophotometer, at room temperature. For solid materials, Agilent CARY 5000 equipment was used to acquire UV-vis diffuse reflectance spectra by applying Kubelka-Munk approach [12]. Shimadzu Instrument model TGA-50 was used to perform the thermogravimetric analysis (TGA), using a heating rate of 20 °C min⁻¹ and argon flow. Chloride potentiometric analysis was performed using AgNO₃ standard solution and a Digimed DM-20 potentiometer equipped with chloride selective electrode. The nitrogen isotherms were determined at 77 K, using a Tristar II Krypton 3020 Micromeritics instrument. Samples were previously degassing at 125 °C, under vacuum for 14 h. BET multipoint method was applied to estimate the surface area. BJH and DFT methods were used to obtain the pore size distributions [41]. Agilent 500 MHz instrument was used to acquire room-temperature ²⁹Si NMR spectra, using CPMAS probe (4 mm) with ~ 10 kHz of spinning rate. TMS was employed as reference for chemical shift. A Nikon D100 camera was used to material pictures. The XPS analysis was performed at LNL Sincrotron Laboratory, using an InSb(111) double-crystal monochromator. The photon energy calibration of monochromator was done at Mo L₁ edge 2866 eV. Additional calibrations were made using gold, 4f_{7/2} peak at 84.0 eV, carbon 1s peak at 284.6 eV and Si 2p peak of SiO₂ at 103.3 eV. The XPS measurements were obtained at a 45° takeoff angle at room temperature. The data were analyzed using the XPSPeak 4.1 software. The peaks were adjusted using a Shirley-type background and an asymmetric Gaussian-Lorentzian sum function (20 % Lorentzian contribution).

2.6. Catalytic performance of SiO₂/SSQ/Au

The alkyne coupling reactions was performed in a sealed reaction tube charged with phenylacetylene (29 μL, 0.25 mmol), 1,10-phenanthroline (18 mg, 0.1 mmol), iodobenzene diacetate (80 mg, 0.25 mmol), gold catalyst (18 mg, 0.22 mol%) in dichloromethane (3 mL). The reaction mixture was stirred at 70 °C for 24 h. As dichloromethane was used as solvent and the reaction was performed above its boiling point in a sealed flask, hypervalent iodine was chosen instead of oxygen from the open atmosphere. The crude reaction mixture was purified by column chromatography using hexane as eluent. All characterization data (¹H NMR and ¹³C NMR spectra) of the organic compounds are presented in Supplementary material (Figures S1-S17).

3. Results and discussion

The SSQ ionic silsesquioxane was grafted onto mesoporous silica

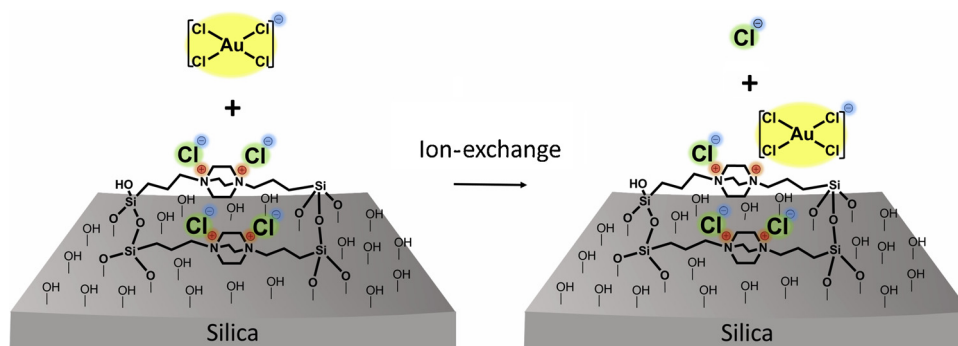


Fig. 1. Representation of silica surface grafted with the ionic silsesquioxane (SiO₂/SSQ) and the ion-exchange process (SiO₂/SSQ/Au).

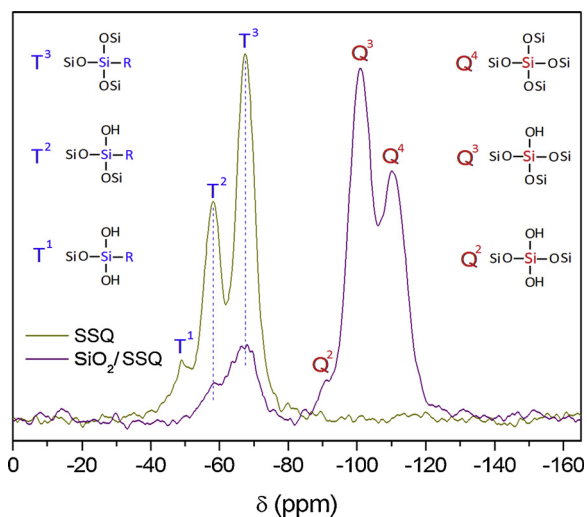


Fig. 2. Solid state MAS ^{29}Si NMR spectra of SSQ ionic silsesquioxane and SiO_2/SSQ material.

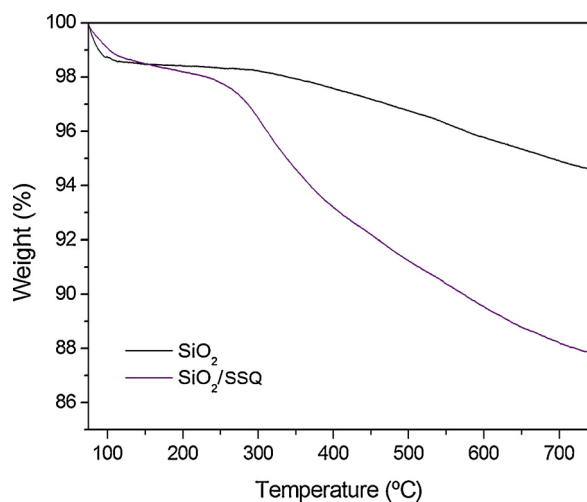


Fig. 3. Thermogravimetric curves for SiO_2 and SiO_2/SSQ materials.

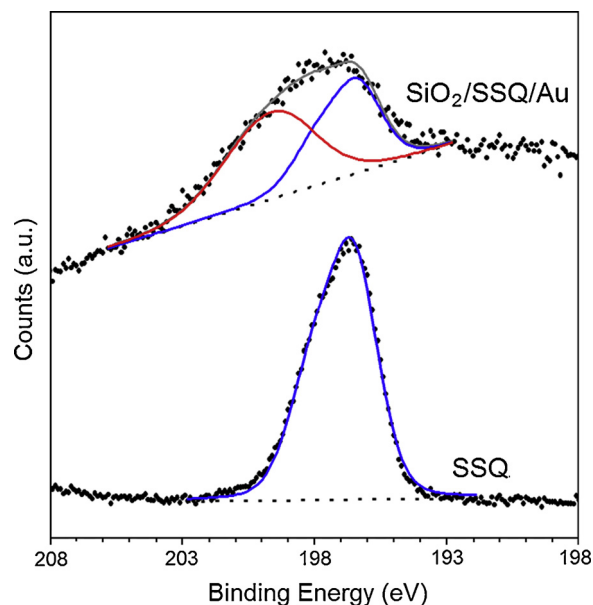


Fig. 5. XPS spectra at the Cl 2p region of the SSQ ionic silsesquioxane and $\text{SiO}_2/\text{SSQ}/\text{Au}$ material. The black points represent the experimental data, the dot line the Shirley background.

xerogel (SiO_2/SSQ) aiming to prepare a support with high surface area to anchor the AuCl_4^- complex ($\text{SiO}_2/\text{SSQ}/\text{Au}$). The modified silica surface and the ion-exchange process are illustrated in Fig. 1.

The ^{29}Si NMR spectra of both SiO_2/SSQ and silsesquioxane materials are presented in Fig. 2. NMR spectrum for silsesquioxane presents three peaks identified as T^3 , T^2 and T^1 silicon species, at -67.5, -58.1 and -49.2 ppm, respectively [12,40]. The spectrum of SiO_2/SSQ enables to observe the occurrence of T^3 and T^2 species coming from the silsesquioxane, as well as, the presence of Q^4 and Q^3 species, at 110 and 100 ppm, respectively, assigned to the silica bulk. These results are clear evidences that silsesquioxane grafting reaction took place on silica surface.

The organofunctionalized silica was submitted to thermogravimetric analysis, and the thermogram is presented in Fig. 3, along with unmodified SiO_2 . The weight loss up to 150 °C is due to water desorption. In the range from 150 to 650 °C, two different processes were observed, silica dehydroxylation reactions and desorption of organic

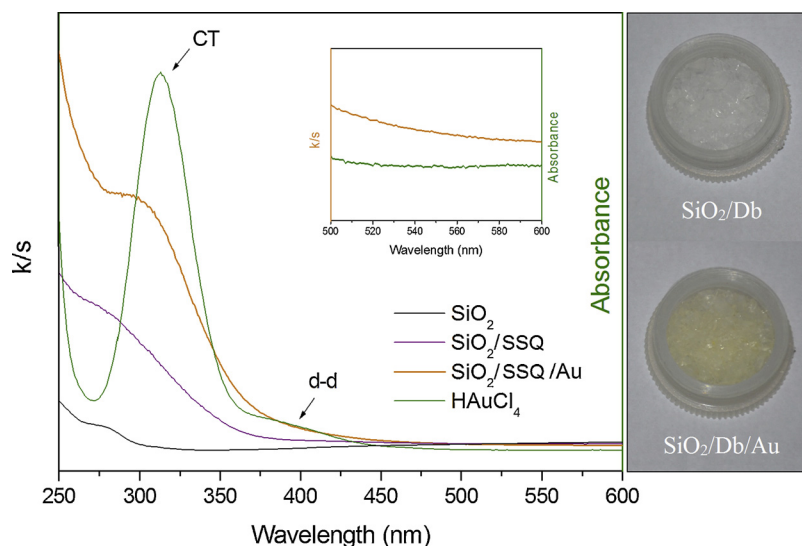


Fig. 4. Absorption profile, k/s calculated from UV-Vis diffuse reflectance spectra of SiO_2 , SiO_2/SSQ and $\text{SiO}_2/\text{SSQ}/\text{Au}$, along with UV-vis spectrum of HAuCl_4 aqueous solution. Inset: spectra of assigned region for plasmon resonance of gold nanoparticle. Aside: photographs of SiO_2/SSQ and $\text{SiO}_2/\text{SSQ}/\text{Au}$ materials.

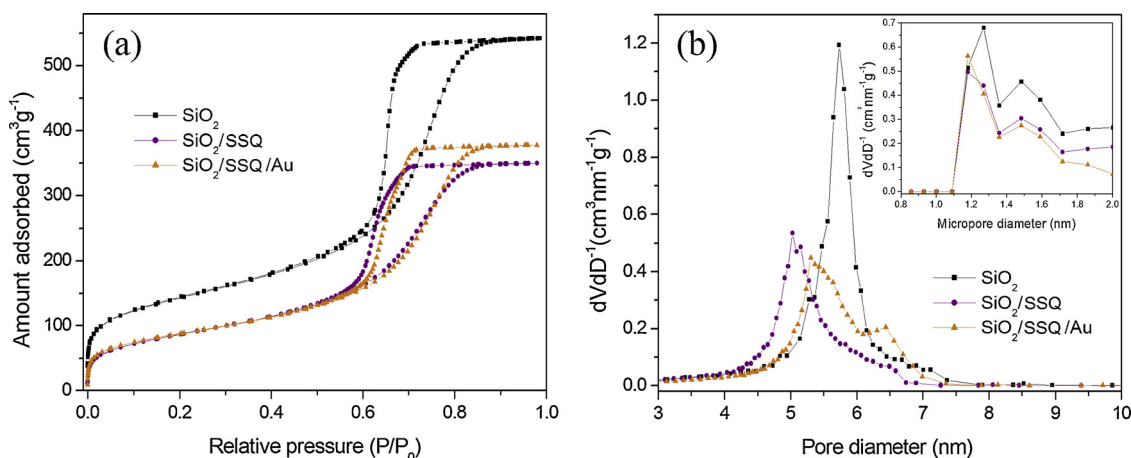


Fig. 6. Textural analysis: (a) N_2 adsorption-desorption isotherms; (b) BJH pore size distribution; Inset Fig. 5b the DFT micropore size distribution.

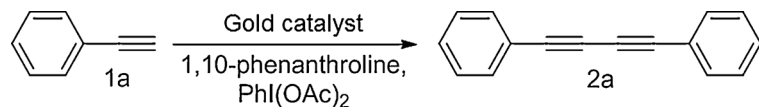
Table 1
Textural analysis.

Sample	Surface area ($\pm 5 \text{ m}^2\text{g}^{-1}$)	Pore volume ($\pm 0.001 \text{ cm}^3\text{g}^{-1}$)
SiO_2	495	0.805
SiO_2/SSQ	313	0.523
$\text{SiO}_2/\text{SSQ}/\text{Au}$	310	0.568

groups. In the case of SiO_2 , the weight loss in this range (3.17 %) is only due to silanol condensation of silica surface. On the other hand, for SiO_2/SSQ material this value was higher (9.68 %) which corresponds not only to dehydroxylation reactions, but also, to decomposition and desorption of SSQ organic groups. Based on these values, the SSQ content was estimated as 0.24 mmol of SSQ groups per gram of SiO_2/SSQ material. It is important to highlight that the SSQ groups grafted on silica surface present good thermal stability, at least until 200 °C. This characteristic of the organofunctionalized support (SiO_2/SSQ) is attractive not only for gold species but for other anionic metal complex as well, in which the catalysis is usually performed below this temperature [42].

The amount of SSQ groups was also estimated by potentiometric analysis through the evaluation of the exchangeable chloride ions. The obtained value was $0.54 \text{ mmol}\cdot\text{g}^{-1}$, corresponding to 0.27 mmol of SSQ

Table 2
Optimization of reaction conditions.



Entry	1,10-phen (equiv)	PhI(OAc) ₂ (equiv)	Temp. (°C)	Time (h)	Solvent	Yield (%)
1	0.4	1.5	25	6	DCM	–
2	0.4	1.5	70	6	DCM	37
3	0.4	1.5	70	18	DCM	99
4	–	1.5	70	24	DCM	4
5	0.4	–	70	24	DCM	–
6 ^a	0.4	–	70	18	DCM	99
7 ^b	0.4	–	70	18	DCM	99
8	0.4	1.5	70	18	MeCN	80
9	0.4	1.5	70	18	HCCl_3	53
10	0.4	1.5	70	18	THF	9
11	0.4	1.5	70	18	EtOH	78
12	0.4	1.0	70	18	DCM	99
13	0.4	0.5	70	18	DCM	54
14	0.2	1.0	70	18	DCM	84

^a diphenyliodonium triflate ((Ph)₂IOTf) as oxidant.

^b bis(trifluoroacetoxy)iodobenzene (PhI(OCOCF₃)₂) as oxidant.

Table 3
Substrates scope for the terminal alkyne homocoupling.

$\text{R}-\text{C}\equiv\text{C}-\text{H} + \text{R}'-\text{C}\equiv\text{C}-\text{H} \xrightarrow[\text{70}^\circ\text{C}, 18\text{h}]{\text{Gold catalyst (0.22 mol\%)} \\ \text{1,10-phenanthroline,} \\ \text{PhI(OAc)}_2, \text{H}_2\text{CCl}_2}$ $\text{R}-\text{C}\equiv\text{C}-\text{C}\equiv\text{C}-\text{R}'$			
Entry	Alkyne	Diyne	Yield
1			2a (99%)
2			2b (90%)
3			2c (92%)
4			2d (63%)
5			2e (74%)
6			2f (70%)
7			2g (30%)
8			2h (99%)
9			2i (91%)

violet region provides the yellowish AuCl_4^- colour (aside of Fig. 4). The nonappearance of band due to plasmon resonance of gold in the nanoparticles form, which usually appears in the range from 500 to 550 nm [12,32] is evidence of its absence. Even more, the $\text{SiO}_2/\text{SSQ}/\text{Au}$ material was annealed at 70°C , which is the temperature that the material was further applied as catalyst and, again, no plasmon resonance band of gold nanoparticles was observed (Supplementary material, Figure S18), therefore confirming the highly dispersed gold complex.

XPS analysis was performed for $\text{SiO}_2/\text{SSQ}/\text{Au}$ material and no peaks of Au 4d (bigger photoionization cross section at $E_{\text{ph}} = 3000\text{ eV}$) or Au 4f regions could be detected, due to the very small gold amount presented in the Supplementary material Figure S19. However, changes in the Cl 2p XPS spectrum of the $\text{SiO}_2/\text{SSQ}/\text{Au}$ material were identified when compared with the Cl 2p XPS spectrum of SSQ ionic silsesquioxane (Fig. 5). The Cl 2p peak of SSQ shows only a single component (blue line), with maximum at 196.7 eV (Fig. 5). This peak corresponds to the chloride ion of SSQ ionic silsesquioxane, as already reported [45]. On the other hand, the Cl 2p peak of $\text{SiO}_2/\text{SSQ}/\text{Au}$ material shows the presence of a new component (Fig. 5). This new component with higher binding energy (red line), which appears around 199.4 eV, is attributed to the chloride from AuCl_4^- complex [46], whose covalent

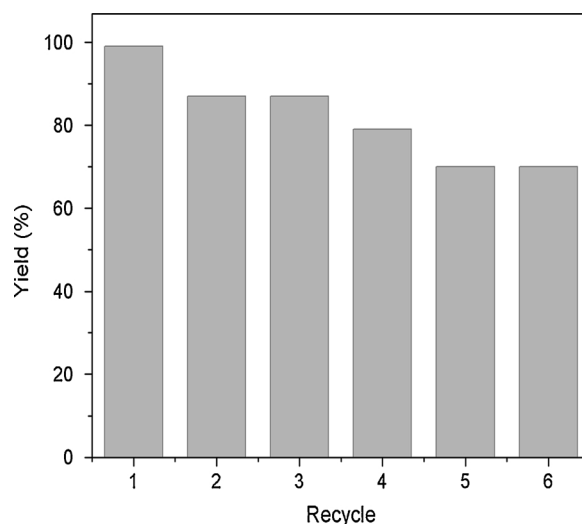
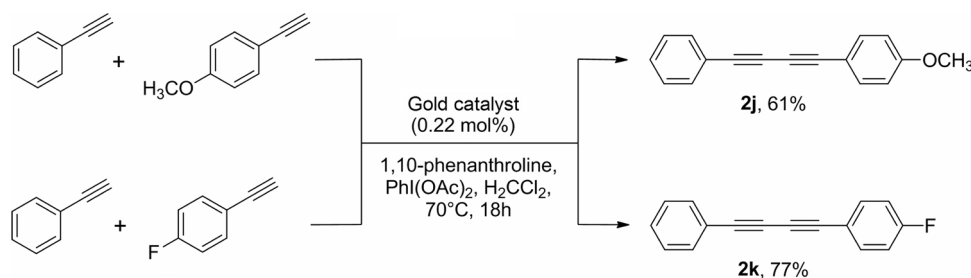


Fig. 7. Recyclability tests of material $\text{SiO}_2/\text{SSQ}/\text{Au}$ for coupling reaction of phenylacetylene under optimized conditions.

character may account for its slightly less anionic behaviour, evidencing the AuCl_4^- species presence in the $\text{SiO}_2/\text{SSQ}/\text{Au}$ material, as attested by UV-vis spectroscopy discussed above.

Fig. 6 shows the textural analysis. The N_2 adsorption/desorption isotherms are presented in Fig. 6a. After the grafting reaction, a decrease in the N_2 adsorption amount is clearly seen in two isotherm regions. The first, in low relative pressures ($P/P_0 < 0.05$), corresponds to micropores and the second one in higher P/P_0 values is related to mesopores [41]. The BJH mesopore size distribution curves are shown in Fig. 6b, in which a sharp peak with maximum around 5.7 nm is clearly observed for SiO_2 material. A shift to lower diameter, with maximum around 5.1 nm, is evident after the grafting reaction with ionic silsesquioxane (SiO_2/SSQ). This shift of 0.6 nm was interpreted considering the presence of polymeric silsesquioxane film on the mesopore surface that also promotes a reduction in BJH mesopore volume, as presented on Table 1. The reduction in the BET surface area after the grafting reaction (Table 1) is mainly produced by trapping of micropores, which are noticed in the DFT micropore distribution curves (inset Fig. 6b).

After the AuCl_4^- adsorption by ion-exchange process ($\text{SiO}_2/\text{SSQ}/\text{Au}$) the isotherms presented very similar profile, although the BJH mesopore curve shows a slight shift to higher diameter values (Fig. 6b). In fact, this feature was already observed in a previous report [47], and it was interpreted as an ionic silsesquioxane leaching process that took place during the ion exchange process. This leaching can produce an erosive process of SiO_2 pore wall. Additionally, the strong acid medium, coming from the HAuCl_4 solution (*aqua regia*), should also contribute to this erosive effect, by converting siloxane to silanol groups, in non-calcined sol-gel silica materials [48]. After the ion exchange process, the surface area value remains the same, while the pore volume underwent a slight increase (Table 1), in agreement with the leaching



Scheme 1. Non-symmetrical diynes.

process proposed above.

Assuming that the ionic gold is uniformly dispersed on the surface, the density of anchored gold “*d*” can be estimated as:

$$d = ([\text{Au}] \times N) / S_{\text{BET}}$$

where “[Au]” is the amount of gold offered (0.03 mmol of AuCl₄[−] per gram of SiO₂/SSQ support), “N” is Avogadro’s number, and S_{BET} is the specific surface area of SiO₂/SSQ material. Thus, the average of inter complex distance; “*ℓ*” is defined as:

$$\ell = (1/d)^{1/2}$$

The found density “*d*” was 0.058 gold complex per square nanometer and therefore, the average distance between them was 4.2 nm, revealing that the gold is really highly dispersed and very far from each other, hindering the gold nanoparticle formation, as shown by UV–vis analysis.

It is important to point out that the SiO₂/SSQ/Au material gathers desirable characteristics to be used as heterogeneous catalyst, such as: i) thermal stability until 70 °C; ii) high dispersion of metal ions, in which every gold atom could be a catalytic site; iii) high surface area, pore volume and pore size that enable fast diffusion and mobility of the species during the catalytic process.

The performance of SiO₂/SSQ/Au material as catalyst was investigated in the oxidative alkyne-alkyne coupling reactions in which the phenylacetylene was selected as the model reaction. The optimal reaction conditions were determined through a series of experiments and the results are summarized in Table 2. First, only 0.22 mol% of the catalyst was used in the dimerization of phenylacetylene (1a), together with 1,10-phenanthroline, di(acetoxyiodo)benzene (PhI(OAc)₂) in dichloromethane (DCM).

No reaction was observed at room temperature after 24 h. The increase in temperature up to 70 °C, in a sealed Schlenk tube, resulted in 37 % yield after 6 h and a complete conversion into the desired 1,3-diyne **2a** occurred after 18 h (Table 2, entries 2–3). The homocoupling did not occur at all if no oxidant (PhI(OAc)₂) or ligand (1,10-phen) is added in the reaction system (Table 2, entries 4–5). Additional experiment in which PhI(OAc)₂ was replaced by diphenyliodonium triflate ((Ph)₂IOTf) or bis(trifluoroacetoxy)iodobenzene (PhI(OCOCF₃)₂) also resulted in full conversion into **2a** (Table 2, entries 6–7), revealing that these other sources of iodonium oxidant are also effective.

The influence of the solvent in the product yield was studied. As can be seen (Table 2, entries 8–11), chloroform, tetrahydrofuran and ethanol were detrimental for the reaction. The amount optimization of both ligand and oxidant (Table 2, entries 12–14) revealed that the best reaction condition consists of 1,10-phenanthroline (0.4 eq.), di(acetoxyiodo)benzene (1.0 eq.) in dichloromethane at 70 °C in closed system. Therefore, this condition was selected to be applied in a new series of reactions where the substrate scope for the terminal alkynes coupling reaction was studied (Table 3). Also, no reaction occurred by using only the SiO₂/SSQ support, without gold in this condition.

Aryl- and alkyl-substituted alkynes were submitted to homo and heterocoupling and resulted in yields from good to high. Functionalized phenylacetylene bearing electron-donating groups [o-NH₂, p-OMe or p-Me] or electron-withdrawing groups (3,5-(CF₃), p-F or p-NO₂) underwent oxidative homocoupling and yielded the corresponding 1,3-diynes in the range from moderate to excellent yields. In case of aliphatic substituted alkynes, different results were observed. While 2-methyl-3-butyn-2-ol resulted in full conversion into product **2h**, only 30 % yield was obtained for **2g**. The procedure was readily extended to the preparation of non-symmetrical diynes by heterocoupling between phenylacetylene **1a** and terminal alkynes **1c** and **1d** using the same optimized conditions. In this case, the heterodiynes **2j** and **2k** (Scheme 1), which are concomitantly formed under these conditions, reaching 61 % and 77 % yields, respectively, were separated from the homodiynes products **2c** and **2d** by column chromatography.

Subsequently, the recyclability of the material SiO₂/SSQ/Au was investigated by means of six repetitions, since it is one of the most important issues from the viewpoint of heterogeneous catalysis. Recycling of the catalyst was performed in a homocoupling reaction using phenylacetylene as model substrate under the optimized conditions. After each cycle, the crude reaction was diluted and the organic phase removed. Reagents were reloaded into the reaction vessel and the next cycle was conducted. The results are shown in Fig. 7.

The catalyst showed an excellent conversion in the first cycle (99 % yield), whereas a slight decrease was observed in the subsequent recycles. This trend was interpreted considering that the catalyst was comminuted by the stirrer, leading to a likely loss of mass. Even though, in the sixth cycle, the reaction yield was still 70 %. Another explanation could be the contribution of the homogeneous catalysis considering the possibility of some gold was leached to the solution. In this way, two additional experiments were performed. Instead of use SiO₂/SSQ/Au material, equal amount of NaAuCl₄ or AuCl were applied under optimized reaction conditions. In both cases, the added salts did not provide the desired 1,3-diyne **2a**, after 18 h. Our assumption is that, in organic media, the gold salt does not present enough solubility to provide the reactive ions or, as the ions become available they could aggregate to form nanoparticles. In both suppositions, deactivation would be expected. In this way, a significant gold leaching from SiO₂/SSQ material was discarded. Consequently, in the applied conditions, our design heterogeneous catalyst is really the responsible by the reaction. Therefore, the SiO₂/SSQ/Au catalyst presents excellent activity and high efficiency concerning the synthetic protocol applied and taking into account the good yields obtained even after six cycles, the possibility of recovering the starting material as well as its simple preparation method.

4. Conclusions

Gold catalyst containing isolated ionic complex sites dispersed on the surface of mesoporous silica was successfully obtained. In order to achieve this purpose, mesoporous silica with sharp pore size distribution, 5.7 nm, was synthesized by sol-gel method. This silica was grafted with ionic silsesquioxane that shows thermal stability up to 200 °C and provides ionic ammonium quaternary sites. This silica modified with ionic groups was used as matrix for ion-exchange immobilization of ionic gold complex. The offered amount of gold was only 12 % of the available exchangeable sites. This small quantity of gold ions provides isolated sites on the matrix surface, with estimated average distance between them of 4.2 nm, hindering the gold aggregation that could lead to the formation of gold nanoparticle, in this way keeping all offered gold as available catalytic sites. The catalyst was efficiently applied in the cross coupling reactions to obtain symmetric and non-symmetric 1,3-diynes, since only 0.22 mol% of the catalyst was sufficient for the coupling reaction. It is important to mention that the reaction system could also be recycled, because good results were obtained even after six reaction runs.

Acknowledgements

We are grateful to CAPES, CNPq, INCT-CMN and FAPERGS for financial and technical support.

Appendix A. Supplementary data

Supplementary material related to this article can be found, in the online version, at doi:<https://doi.org/10.1016/j.apcata.2020.117444>.

References

- [1] T. Li, F. Liu, Y. Tang, L. Li, S. Miao, Y. Su, J. Zhang, J. Huang, H. Sun, M. Haruta, A. Wang, B. Qiao, J. Li, T. Zhang, *Angew. Chem. Int. Ed.* 57 (2018) 7795–7799,

- <https://doi.org/10.1002/anie.201803272>.
- [2] G.C. Bond, *Molecules* 17 (2012) 1716–1743, <https://doi.org/10.3390/molecules17021716>.
- [3] J. Oliver-Meseguer, J.R. Cabrero-Antonino, I. Domínguez, A. Leyva-Pérez, A. Corma, *Science* 338 (2012) 1452–1455, <https://doi.org/10.1126/science.1227813>.
- [4] J. Lin, H. Abroshan, C. Liu, M. Zhu, G. Li, M. Haruta, *J. Catal.* 330 (2015) 354–436, <https://doi.org/10.1016/j.jcat.2015.07.020>.
- [5] M.C.B. Jaimes, F. Rominger, M.M. Pereira, R.M.B. Carrilho, S.A.C. Carabineiro, A.S.K. Hashmi, *Chem. Commun.* 50 (2014) 4937–4940, <https://doi.org/10.1039/c4cc00839a>.
- [6] Z. Cao, D.M. Bassani, B. Bibal, *Chem. Eur. J.* 24 (2018) 18779–18787, <https://doi.org/10.1002/chem.201804322>.
- [7] Z. Wu, M.A. MacDonald, J. Chen, P. Zhang, R. Jin, *J. Am. Chem. Soc.* 133 (2011) 9670–9673, <https://doi.org/10.1021/ja2028102>.
- [8] D.K. Mishra, J.K. Cho, Y. Yi, H.J. Lee, Y.J. Kim, *J. Ind. Eng. Chem.* 70 (2019) 338–345, <https://doi.org/10.1016/j.jiec.2018.10.034>.
- [9] Z. Ma, S. Dai, *Nano Res.* 4 (2011) 3–32, <https://doi.org/10.1007/s12274-010-0025-5>.
- [10] C.W. Corti, R.J. Holliday, D.T. Thompson, *Appl. Catal. A Gen.* 291 (2005) 253–261, <https://doi.org/10.1016/j.apcata.2005.01.051>.
- [11] G. Li, D. Jiang, C. Liu, C. Yu, R. Jin, *J. Catal.* 306 (2013) 177–183, <https://doi.org/10.1016/j.jcat.2013.06.017>.
- [12] C.A. Didó, C.D.G. Caneppele, A.C. Schneid, M.B. Pereira, T.M.H. Costa, E.V. Benvenutti, *Microporous Mesoporous Mater.* 270 (2018) 48–56, <https://doi.org/10.1016/j.micromeso.2018.04.047>.
- [13] M. Deon, R.C. de Andrade, S. Nicolodi, J.B.M. da Cunha, T.M.H. Costa, F.S. Rodembusch, E.W. de Menezes, E.V. Benvenutti, *Part. Part. Syst. Charact.* 35 (2018) 1800160, <https://doi.org/10.1002/ppsc.201800160>.
- [14] R. Ciriminna, A. Fidalgo, V. Pandarus, F. Bédard, L.M. Ilharco, M. Pagliaro, *Chem. Rev.* 113 (2013) 6592–6620, <https://doi.org/10.1021/cr300399c>.
- [15] L.-F. Gutiérrez, S. Hamoudi, K. Belkacemi, *Catalysts* 1 (2011) 97–154, <https://doi.org/10.3390/catal1010097>.
- [16] L.V. de Souza, O. Tkachenko, B.N. Cardoso, T.M. Pizzolato, S.L.P. Dias, M.A.Z. Vasconcellos, L.T. Arenas, T.M.H. Costa, C.C. Moro, E.V. Benvenutti, *Microporous Mesoporous Mater.* 287 (2019) 203–210, <https://doi.org/10.1016/j.micromeso.2019.06.013>.
- [17] R. Dorel, A.M. Echavarren, *Chem. Rev.* 115 (2015) 9028–9072, <https://doi.org/10.1021/cr500691k>.
- [18] A.M. Asiria, A.S.K. Hashmi, *Chem. Soc. Rev.* 45 (2016) 4471–4503, <https://doi.org/10.1039/C6CS00023A>.
- [19] Y. Yang, J. Schiefl, S. Zallouz, V. Göker, J. Gross, M. Rudolph, F. Rominger, A.S.K. Hashmi, *Chem. Eur. J.* 25 (2019) 9624–9628, <https://doi.org/10.1002/chem.201902213>.
- [20] A.L. Pérez, A. Doménech, S. Al-Resayes, A. Corma, *ACS Catal.* 2 (2012) 121–126, <https://doi.org/10.1021/cs200532c>.
- [21] H. Peng, Y. Xi, N. Ronaghi, B. Dong, N.G. Akhmedov, X. Shi, *J. Am. Chem. Soc.* 136 (2014) 13174–13177, <https://doi.org/10.1021/ja5078365>.
- [22] W. Shi, A. Lei, *Tetrahedron Lett.* 55 (2014) 2763–2772, <https://doi.org/10.1016/j.tetlet.2014.03.022>.
- [23] S. Banerjee, N.T. Patil, *Chem. Commun.* 53 (2017) 7937–7940, <https://doi.org/10.1039/C7CC04283C>.
- [24] Z. Xia, V. Corcé, F. Zhao, C. Przybylski, A. Espagne, L. Jullien, T. Le Saux, Y. Gimbert, H. Dossmann, V. Mouriers-Mansuy, C. Ollivier, L. Fensterbank, *Nat. Chem. Biol.* 11 (2019) 797–805, <https://doi.org/10.1038/s41557-019-0295-9>.
- [25] P.J.G. Goulet, R.B. Lennox, *J. Am. Chem. Soc.* 132 (2010) 9582–9584, <https://doi.org/10.1021/ja104011b>.
- [26] G. Li, R. Jin, *Nanotechnol. Rev.* 2 (2013) 529–545, <https://doi.org/10.1515/ntrev-2013-0020>.
- [27] M. Hofer, T. de Haro, E. Gómez-Bengoia, A. Genoux, C. Nevado, *Chem. Sci.* 10 (2019) 8411–8420, <https://doi.org/10.1039/c9sc02372k>.
- [28] J.H. Teles, *Angew. Chem. Int. Ed.* 54 (2015) 5556–5558, <https://doi.org/10.1002/anie.201501966>.
- [29] B. Ranieri, I. Escofet, A.M. Echavarren, *Org. Biomol. Chem.* 13 (2015) 7103–7118, <https://doi.org/10.1039/c5ob00736d>.
- [30] J. Rodríguez, N. Adet, N. Saffon-Merceron, D. Bourissou, *Chem. Commun.* 56 (2020) 94–97, <https://doi.org/10.1039/c9cc07666b>.
- [31] C. Engelbrekt, P.S. Jensen, K.H. Sørensen, J. Ulstrup, J. Zhang, *J. Phys. Chem. C* 117 (2013) 11818–11828, <https://doi.org/10.1021/jp401883h>.
- [32] A.H. Virgili, L. Luza, J.A. Fernandes, T.M.H. Costa, E.W. de Menezes, E.V. Benvenutti, *Catal. Commun.* 166 (2018) 32–37, <https://doi.org/10.1016/j.catcom.2018.08.003>.
- [33] P. Wu, P. Bai, Z. Lei, K.P. Loh, X.S. Zhao, *Microporous Mesoporous Mater.* 141 (2020) 222–230, <https://doi.org/10.1016/j.micromeso.2010.11.011>.
- [34] B. Lee, Z. Ma, Z. Zhang, C. Park, S. Dai, *Microporous Mesoporous Mater.* 122 (2009) 160–167, <https://doi.org/10.1016/j.micromeso.2009.02.029>.
- [35] G.R.S. Andrade, C.C. Nascimento, Y.H. Santos, L.P. Costa, L.E. Almeida, I.F. Gimenez, *Dyes Pigm.* 155 (2018) 202–211, <https://doi.org/10.1016/j.dyepig.2018.03.052>.
- [36] C.H. Campos, B.F. Urbano, B.L. Rivas, *Mater. Lett.* 131 (2014) 198–202, <https://doi.org/10.1016/j.matlet.2014.05.161>.
- [37] B.M. Barngrover, C.M. Aikens, *J. Phys. Chem. A* 117 (2013) 5377–5384, <https://doi.org/10.1021/jp403633a>.
- [38] C.H. Campos, B.F. Urbano, C.C. Torres, J.A. Alderete, *J. Chem.* (2017) 7941853, <https://doi.org/10.1155/2017/7941853>.
- [39] Y. Gushikem, E.V. Benvenutti, Y.V. Kholin, *Pure Appl. Chem.* 80 (2008) 1593–1611, <https://doi.org/10.1351/pac200880071593>.
- [40] L.T. Arenas, A.C. Pinheiro, J.D. Ferreira, P.R. Livotto, V.P. Pereira, M.R. Gallas, Y. Gushikem, T.M.H. Costa, E.V. Benvenutti, *J. Colloid Interface Sci.* 318 (2008) 96–102, <https://doi.org/10.1016/j.jcis.2007.09.073>.
- [41] S.J. Gregg, K.S.W. Sing, *Adsorption, Surface Area and Porosity*, 2nd ed., Academic Press, London, 1982.
- [42] G. Kratošová, V. Holířová, Z. Konvičková, A.P. Ingle, S. Gaikwad, K. Škrlavá, A. Prokop, M. Rai, D. Plachá, *Biotechnol. Adv.* 37 (2019) 154–176, <https://doi.org/10.1016/j.biotechadv.2018.11.012>.
- [43] A.K. Gangopadhyay, A. Chakravorty, *J. Chem. Phys.* 35 (1961) 2206–2209, <https://doi.org/10.1063/1.1732233>.
- [44] B. Streszewski, W. Jaworski, K. Szaciłowski, K. Paclawski, *Int. J. Chem. Kinet.* 46 (2014) 328–337, <https://doi.org/10.1002/kin.20850>.
- [45] M.R. Nunes, Y. Gushikem, R. Landers, J. Dupont, E.V. Benvenutti, *J. Sol-Gel Sci. Technol.* 63 (2012) 258–265, <https://doi.org/10.1007/s10971-012-2696-8>.
- [46] C. Zhao, B. Ren, Y. Song, J. Zhang, L. Wei, S. Chen, S. Zhang, *RSC Adv.* 4 (2014) 16267–16273, <https://doi.org/10.1039/C4RA00569D>.
- [47] M. Deon, E.M. Caldas, D.S. Rosa, E.W. de Menezes, S.L.P. Dias, M.B. Pereira, T.M.H. Costa, L.T. Arenas, E.V. Benvenutti, *J. Solid State Electrochem.* 19 (2015) 2095–2105, <https://doi.org/10.1007/s10008-014-2687-5>.
- [48] R.K. Iler, *The Chemistry of Silica*, John Wiley & Sons, New York, 1979.